

## CHARACTERISTICS OF GUIDED MODES IN UNIAXIAL CHIRAL CIRCULAR WAVEGUIDES

J.-F. Dong\* and J. Li

Institute of Optical Fiber Communication and Network Technology,  
Ningbo University, Ningbo 315211, China

**Abstract**—The characteristics of guided modes in the circular waveguide consist of uniaxial chiral medium have been investigated. The characteristic equation of guided modes is derived. The dispersion curves and energy flux of guided modes for three kinds of uniaxial chiral media are presented. Unusual dispersion characteristics and negative energy flux are found, i.e., backward wave is supported in the uniaxial chiral waveguide.

### 1. INTRODUCTION

In recent years, chiral metamaterials have attracted much attention because the negative refractive index can be realized in the chiral metamaterials [1–9] and because a chiral slab with negative refractive index can be used as a perfect lens which providing subwavelength resolution for circularly polarized waves [10, 11]. Surface polaritons [12] and Goos-Hanchen shift [13] at the surface of chiral negative refractive media have been studied. Waveguides consisting of chiral metamaterials with negative refractive indices, such as slab, grounded slab, parallel-plate waveguide and fiber, have been investigated theoretically [14–17]. A special case of chiral negative refractive index medium, termed as chiral nihility [1] in which the permittivity and permeability are simultaneously zero, has also intensively explored [18–30]. Especially, planar and circular open [18, 20–24, 29] or closed [30] waveguides containing chiral nihility have been studied. However, these studies focus on the isotropic chiral medium. Usually, uniaxially anisotropic chiral media are quite easy to be realized artificially [31]. Recently, Cheng and Cui [31, 32] investigated negative refractions in

---

*Received 23 November 2011, Accepted 19 January 2012, Scheduled 30 January 2012*

\* Corresponding author: Jian-Feng Dong (dongjianfeng@nbu.edu.cn).

uniaxially anisotropic chiral media. They found that the condition to realize the negative refraction in uniaxial chiral media can be quite loose. Mahmoud and Viitanen [33] considered propagation of waves in uniaxial chiral circular waveguide with boundary condition of hard surface. However, the possibility of negative electromagnetic parameter and negative refractive index has not been discussed in [33]. Guided modes in open circular waveguides (fibers) consisting of isotropic chiral media [17, 34, 35] or negative index materials [36] have been studied in the literature. Slab or planar waveguides consisting of uniaxial anisotropic non-chiral media have also been examined [37, 38]. In our previous papers, novel characteristics of guided modes in the isotropic chiral negative refractive index fiber [17] and chiral nihility fiber [22, 23] have been investigated. In this paper, we extend these studies into open circular waveguides consisting of uniaxial chiral media with negative electromagnetic parameters. Firstly, we derive the characteristic equation of guided modes, then present numerical results of low-order guided modes for three kinds of uniaxial chiral media: I  $\varepsilon_t > 0$ ,  $\varepsilon_z > 0$ , II  $\varepsilon_t < 0$ ,  $\varepsilon_z > 0$ , and III  $\varepsilon_t > 0$ ,  $\varepsilon_z < 0$ , among which there are no counterparts in isotropic chiral case and relative easily realized (see Fig. 1 in [31]), and we also discuss the effects of chirality parameter on dispersion characteristics and energy flux.

## 2. MODAL CHARACTERISTIC EQUATION

Consider the circular waveguide in which the core is uniaxial chiral medium and cladding is conventional material. The radius of core is  $a$ . The cladding is assumed to extend infinitely. Here we adopt the cylindrical coordinate system  $(r, \varphi, z)$  and time-harmonic field with  $\exp(j\omega t)$ .

The constitutive relations in the uniaxial chiral medium are [39]:

$$\mathbf{D} = [\varepsilon_t \bar{\bar{I}}_t + \varepsilon_z \hat{\mathbf{z}}\hat{\mathbf{z}}] \cdot \mathbf{E} - j\kappa \sqrt{\mu_0 \varepsilon_0} \hat{\mathbf{z}}\hat{\mathbf{z}} \cdot \mathbf{H} \quad (1)$$

$$\mathbf{B} = [\mu_t \bar{\bar{I}}_t + \mu_z \hat{\mathbf{z}}\hat{\mathbf{z}}] \cdot \mathbf{H} + j\kappa \sqrt{\mu_0 \varepsilon_0} \hat{\mathbf{z}}\hat{\mathbf{z}} \cdot \mathbf{E} \quad (2)$$

where  $\varepsilon_t$  ( $\mu_t$ ) and  $\varepsilon_z$  ( $\mu_z$ ) are permittivity (permeability) of the uniaxial chiral medium in transversal and longitudinal direction, respectively;  $\varepsilon_0$  and  $\mu_0$  are permittivity and permeability of free space.  $\kappa$  is the chirality parameter, which describes electromagnetic coupling.  $\hat{\mathbf{z}}$  is a unit vector along the waveguide axis (longitudinal direction) and  $\bar{\bar{I}}_t = \hat{\mathbf{x}}\hat{\mathbf{x}} + \hat{\mathbf{y}}\hat{\mathbf{y}}$ .

By separating the modal fields in the waveguide into transversal and longitudinal electromagnetic field components, we obtain:

$$\mathbf{E} = (\mathbf{E}_t + E_z \hat{\mathbf{z}}) \exp(-j\beta z) \tag{3}$$

$$\mathbf{H} = (\mathbf{H}_t + H_z \hat{\mathbf{z}}) \exp(-j\beta z) \tag{4}$$

where  $\beta$  is the longitudinal propagation constant. According to Maxwell's equations and above constitutive relations, the relationships between the transversal and longitudinal electromagnetic field components can be derived as follows:

$$\mathbf{E}_t = -j \frac{\beta}{\lambda^2} \nabla_t E_z - j \frac{\omega \mu_t}{\lambda^2} \nabla_t H_z \times \hat{\mathbf{z}} \tag{5}$$

$$\mathbf{H}_t = -j \frac{\beta}{\lambda^2} \nabla_t H_z - j \frac{\omega \varepsilon_t}{\lambda^2} \hat{\mathbf{z}} \times \nabla_t E_z \tag{6}$$

where  $\nabla_t = \nabla - \hat{\mathbf{z}} \frac{\partial}{\partial z}$ ,  $\lambda^2 = \omega^2 \mu_t \varepsilon_t - \beta^2$ , and longitudinal electromagnetic field components satisfy wave equations [33]:

$$\begin{bmatrix} \nabla_t^2 E_z \\ \nabla_t^2 H_z \end{bmatrix} + \lambda^2 \begin{bmatrix} \varepsilon_z / \varepsilon_t & -j \kappa \sqrt{\varepsilon_0 \mu_0} / \varepsilon_t \\ j \kappa \sqrt{\varepsilon_0 \mu_0} / \mu_t & \mu_z / \mu_t \end{bmatrix} \begin{bmatrix} E_z \\ H_z \end{bmatrix} = 0 \tag{7}$$

By finding the eigenvectors and eigenvalues of the  $2 \times 2$  matrix in Equation (7), one can obtain the modal field structure [33]. The eigenvalues  $k_c^2$  of  $2 \times 2$  matrix in Equation (7) have two values:

$$k_{c\pm}^2 = \frac{\lambda^2}{2} \left[ \frac{\varepsilon_z}{\varepsilon_t} + \frac{\mu_z}{\mu_t} \pm \sqrt{\left( \frac{\varepsilon_z}{\varepsilon_t} - \frac{\mu_z}{\mu_t} \right)^2 + 4 \kappa^2 \frac{\varepsilon_0 \mu_0}{\varepsilon_t \mu_t}} \right] \tag{8}$$

The corresponding eigenfunctions are given by [33]:

$$(E_z, H_z) = \left( E_z, j \frac{\alpha}{\eta_t} E_z \right) \tag{9}$$

where  $\alpha = \left( \frac{k_c^2}{\lambda^2} - \frac{\varepsilon_z}{\varepsilon_t} \right) \sqrt{\varepsilon_t \mu_t} / (\kappa \sqrt{\varepsilon_0 \mu_0})$ ,  $\eta_t = \sqrt{\mu_t / \varepsilon_t}$ .

Thus the wave equation of the longitudinal electromagnetic field component  $E_z$  becomes

$$\nabla_t^2 E_z + k_c^2 E_z = 0 \tag{10}$$

In the cylindrical coordinate system  $(r, \varphi, z)$ , the solution of the longitudinal electromagnetic field component in the core has the form  $E_z = J_m(k_c r) \exp(jm\varphi)$ . Then the total longitudinal electromagnetic field components in the core can be written as

$$E_{z1} = [A_m J_m(k_{c+} r) + B_m J_m(k_{c-} r)] \exp(jm\varphi) \exp(-j\beta z) \tag{11a}$$

$$H_{z1} = \frac{j}{\eta_t} [A_m \alpha_+ J_m(k_{c+} r) + B_m \alpha_- J_m(k_{c-} r)] \exp(jm\varphi) \exp(-j\beta z) \tag{11b}$$

The transversal electromagnetic field components can be derived from Equations (5), (6) as:

$$E_{r1} = \left\{ A_m \left[ \frac{jm k_t}{\lambda^2 r} \alpha_+ J_m(k_{c+r}) - \frac{j\beta k_{c+}}{\lambda^2} J'_m(k_{c+r}) \right] + B_m \left[ \frac{jm k_t}{\lambda^2 r} \alpha_- J_m(k_{c-r}) - \frac{j\beta k_{c-}}{\lambda^2} J'_m(k_{c-r}) \right] \right\} \exp(jm\varphi) \exp(-j\beta z) \quad (11c)$$

$$E_{\varphi 1} = \left\{ A_m \left[ \frac{m\beta}{\lambda^2 r} J_m(k_{c+r}) - \frac{k_t k_{c+} \alpha_+}{\lambda^2} J'_m(k_{c+r}) \right] + B_m \left[ \frac{m\beta}{\lambda^2 r} J_m(k_{c-r}) - \frac{k_t k_{c-} \alpha_-}{\lambda^2} J'_m(k_{c-r}) \right] \right\} \exp(jm\varphi) \exp(-j\beta z) \quad (11d)$$

$$H_{r1} = \left\{ A_m \frac{1}{\lambda^2 \eta_t} \left[ -\frac{k_t m}{r} J_m(k_{c+r}) + \beta k_{c+} \alpha_+ J'_m(k_{c+r}) \right] + B_m \frac{1}{\lambda^2 \eta_t} \left[ -\frac{k_t m}{r} J_m(k_{c-r}) + \beta k_{c-} \alpha_- J'_m(k_{c-r}) \right] \right\} \exp(jm\varphi) \exp(-j\beta z) \quad (11e)$$

$$H_{\varphi 1} = \left\{ A_m \frac{1}{\lambda^2 \eta_t} \left[ \frac{j\beta m \alpha_+}{r} J_m(k_{c+r}) - k_t k_{c+} J'_m(k_{c+r}) \right] + B_m \frac{1}{\lambda^2 \eta_t} \left[ \frac{j\beta m \alpha_-}{r} J_m(k_{c-r}) - k_t k_{c-} J'_m(k_{c-r}) \right] \right\} \exp(jm\varphi) \exp(-j\beta z) \quad (11f)$$

where  $A_m$ ,  $B_m$  are constants,  $J_m(\cdot)$  the Bessel function of first kind,  $J'_m(\cdot)$  the differentiation with respect to argument, and  $m$  a positive or negative integer specifying the azimuthal field dependence.

In the cladding, the electromagnetic fields can be obtained as [22]:

$$\begin{cases} E_{z2} = C_m K_m(\tau_2 r) \exp(jm\varphi) \exp(-j\beta z) \\ H_{z2} = \frac{j}{\eta_2} D_m K_m(\tau_2 r) \exp(jm\varphi) \exp(-j\beta z) \end{cases} \quad (12a)$$

$$\begin{cases} E_{r2} = \left[ \frac{j\beta}{\tau_2} C_m K'_m(\tau_2 r) - \frac{jm k_2}{\tau_2^2 r} D_m K_m(\tau_2 r) \right] \exp(jm\varphi) \exp(-j\beta z) \\ H_{r2} = \left[ \frac{m k_2}{\eta_2 \tau_2^2 r} C_m K_m(\tau_2 r) - \frac{\beta}{\eta_2 \tau_2} D_m K'_m(\tau_2 r) \right] \exp(jm\varphi) \exp(-j\beta z) \end{cases} \quad (12b)$$

$$\begin{cases} E_{\varphi 2} = \left[ -\frac{m\beta}{\tau_2^2 r} C_m K_m(\tau_2 r) + \frac{k_2}{\tau_2} D_m K'_m(\tau_2 r) \right] \exp(jm\varphi) \exp(-j\beta z) \\ H_{\varphi 2} = \left[ \frac{jk_2}{\eta_2 \tau_2} C_m K'_m(\tau_2 r) - \frac{jm\beta}{\eta_2 \tau_2^2 r} D_m K_m(\tau_2 r) \right] \exp(jm\varphi) \exp(-j\beta z) \end{cases} \quad (12c)$$

where  $C_m$ ,  $D_m$  are constants,  $K_m(\cdot)$  the modified Bessel function of second kind, and  $K'_m(\cdot)$  the differentiation with respect to argument,

$\tau_2 = \sqrt{\beta^2 - k_2^2}$  the transverse attenuation factor in the cladding;  $k_2 = \omega\sqrt{\mu_2\varepsilon_2}$ , and  $\eta_2 = \sqrt{\mu_2/\varepsilon_2}$  the wavenumber and wave impedance in the cladding, respectively.

According to four boundary conditions (continuity of the tangential electromagnetic field components  $E_z, E_\varphi, H_z, H_\varphi$ ) at interface  $r = a$ , the following equation can be derived:

$$\begin{bmatrix} J_m(u_+) & J_m(u_-) & -K_m(v) & 0 \\ \alpha_+ J_m(u_+) & \alpha_- J_m(u_-) & 0 & -\frac{\eta_t}{\eta_2} K_m(v) \\ a_{31} & a_{32} & \frac{m\beta}{\tau_2^2 a} K_m(v) & -\frac{k_2}{\tau_2} K'_m(v) \\ a_{41} & a_{42} & -\frac{\eta_t}{\eta_2} \frac{k_2}{\tau_2} K'_m(v) & \frac{\eta_t}{\eta_2} \frac{m\beta}{\tau_2^2 a} K_m(v) \end{bmatrix} \begin{bmatrix} A_m \\ B_m \\ C_m \\ D_m \end{bmatrix} = 0 \quad (13)$$

where  $a_{31} = \frac{m\beta}{\lambda^2 a} J_m(u_+) - \frac{\omega\mu_t k_{c+} \alpha_+}{\eta_t \lambda^2} J'_m(u_+)$ ,  $a_{32} = \frac{m\beta}{\lambda^2 a} J_m(u_-) - \frac{\omega\mu_t k_{c-} \alpha_-}{\eta_t \lambda^2} J'_m(u_-)$ ,  $a_{41} = \frac{m\beta \alpha_+}{\lambda^2 a} J_m(u_+) - \frac{\omega\varepsilon_t \eta_t k_{c+}}{\lambda^2} J'_m(u_+)$ ,  $a_{42} = \frac{m\beta \alpha_-}{\lambda^2 a} J_m(u_-) - \frac{\omega\varepsilon_t \eta_t k_{c-}}{\lambda^2} J'_m(u_-)$ , and  $u_\pm = k_{c\pm} a$ ,  $v = \tau_2 a$ . The characteristic equation of guided modes is simply given as determinant of  $4 \times 4$  matrix in (13) equal to zero.

Energy flux along the  $z$ -axis in the waveguide is defined by:

$$S_z = \frac{1}{2} \text{Re}(\mathbf{E} \times \mathbf{H}^*) \cdot \hat{\mathbf{z}} = \frac{1}{2} \text{Re}(E_r H_\varphi^* - E_\varphi H_r^*) \quad (14)$$

Power in the core ( $P_1$ ) and cladding ( $P_2$ ) are the integration of the energy flux  $S_{z1}$  and  $S_{z2}$ , respectively:

$$P_1 = \int_0^{2\pi} \int_0^a r S_{z1} dr d\varphi = 2\pi \int_0^a r S_{z1} dr \quad (15a)$$

$$P_2 = \int_0^{2\pi} \int_a^\infty r S_{z2} dr d\varphi = 2\pi \int_a^\infty r S_{z2} dr \quad (15b)$$

The normalized power is defined as [36]

$$P = \frac{P_1 + P_2}{|P_1| + |P_2|} \quad (16)$$

### 3. NUMERICAL RESULTS AND DISCUSSION

The longitudinal propagation constant  $\beta$  can be calculated numerically from the characteristic equation, and relationships of constants  $A_m, B_m, C_m$ , and  $D_m$  in the formulas of electromagnetic fields can be derived from Equation (13). Thus all electromagnetic fields components, the energy flow distribution and normalized power can be obtained. In this section, we will present the dispersion curves, energy flux of guided modes for three kinds of uniaxial chiral media [31, 32]:

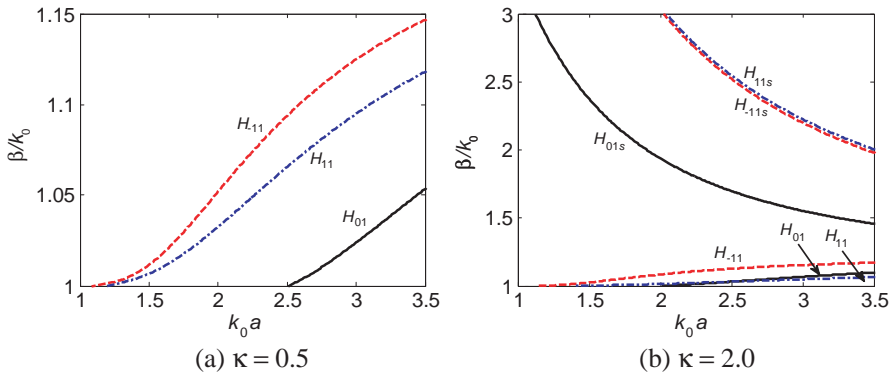


**Figure 1.** Dispersion curves of lower-order ( $m = -1, 0, 1$ ) guided modes for different chirality parameters.

$\varepsilon_t > 0, \varepsilon_z > 0$ ;  $\varepsilon_t < 0, \varepsilon_z > 0$ ; and  $\varepsilon_t > 0, \varepsilon_z < 0$ . Here we assume  $\mu_t = \mu_z = \mu_0$ , use normalized frequency  $k_0a$ , and focus on the lower-order ( $m = -1, 0, 1$ ) guided modes.

### 3.1. Case I: $\varepsilon_t > 0, \varepsilon_z > 0$

We choose  $\varepsilon_t = 1.5\varepsilon_0, \varepsilon_z = 2.5\varepsilon_0$ . For small and middle value of chirality parameter  $\kappa$ , the dispersion curves are similar as isotropic chiral circular waveguides [34, 35], as shown in Fig. 1(a) for  $\kappa = 0.5$ . The normalized propagation constants  $\beta/k_0$  of  $H_{-11}$  mode (dashed curve) and  $H_{11}$  mode (dash-dotted curve) are different, and increase as normalized frequency  $k_0a$  increases. The fundamental mode is  $H_{-11}$  mode. For larger value of chirality parameter  $\kappa$ , another type of mode (label as  $H_{mms}$ ) with negative slope shape appears, as shown in Fig. 1(b) for  $\kappa = 2.0$ . The normalized propagation constants  $\beta/k_0$  of these modes ( $H_{01s}, H_{-11s}, H_{11s}$  modes) are always larger than  $\sqrt{\varepsilon_t/\varepsilon_0} = 1.225$ . For a fixed normalized frequency  $k_0a$ , the value of  $\beta/k_0$  of  $H_{01s}$  mode (solid curve) is smaller than those of  $H_{-11s}$  and  $H_{11s}$  modes.

In order to clearly investigate the propagation of electromagnetic wave in the waveguide, the energy flux  $S_z$  of guided modes in radial direction is examined. Fig. 2 shows normalized energy flux  $S_z$  of  $H_{01}, H_{-11}, H_{11}$  modes for  $\kappa = 0.5$  at normalized frequency  $k_0a = 3$ . They are all positive in the core and cladding. The maximum of energy flux  $S_z$  is located in the middle of the core for  $H_{01}$  mode and in the center of the core for  $H_{-11}$  and  $H_{11}$  modes. However, for another type of mode, there are negative energy flux  $S_z$  near the center for  $H_{-11s}$  mode and in the middle for  $H_{11s}$  mode (see Fig. 3). The energy flux  $S_z$

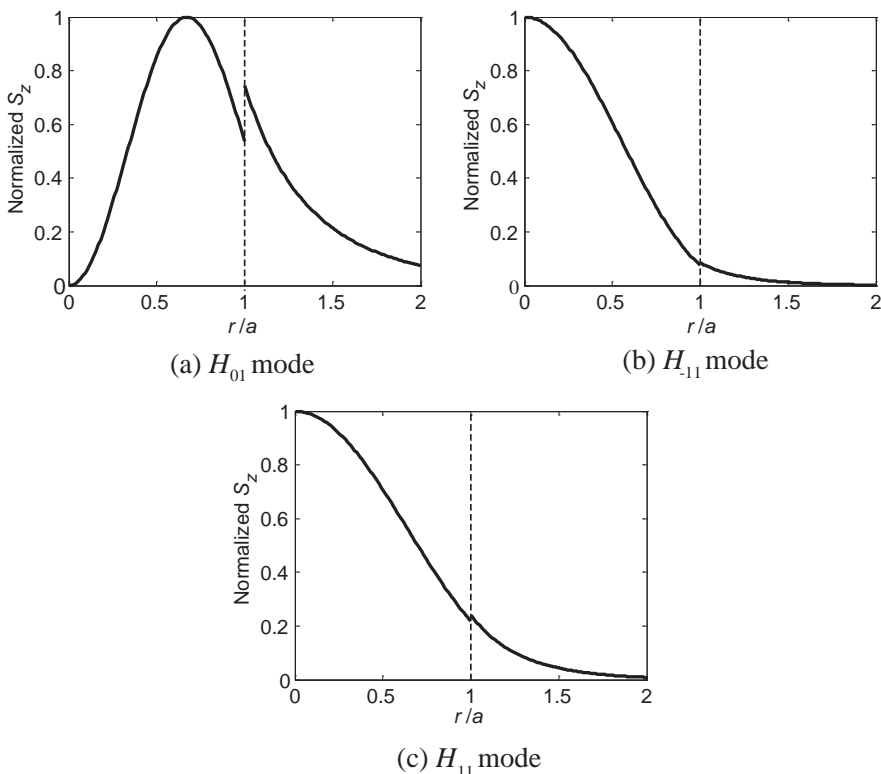


**Figure 2.** Normalized energy flux  $S_z$  of modes for  $\kappa = 0.5$  at  $k_0a = 3$ .

in the core changes sign for  $H_{-11s}$  mode and changes sign two times for  $H_{11s}$  mode at  $k_0a = 2$ . For  $H_{11s}$  mode, at small normalized frequency  $k_0a$ , the energy flux  $S_z$  becomes negative near interface, even in the cladding (Fig. 4). This is a novel phenomenon.

It is found from calculation that the normalized power  $P$  of all guided modes (including  $H_{mns}$  modes) are positive, although power in the cladding can be negative in some cases (for example in Fig. 4, the value of normalized power is smaller than one), thus they are forward waves, which means that the flow of the power is parallel to wave vector propagation direction.

### 3.2. Case II: $\varepsilon_t < 0, \varepsilon_z > 0$

We choose  $\varepsilon_t = -\varepsilon_0, \varepsilon_z = 2\varepsilon_0$ . Fig. 5 shows the dispersion curves of  $H_{01s}, H_{-11s}, H_{11s}, H_{02s}, H_{-12s}, H_{12s}$  modes for  $\kappa = 0.5$  and  $\kappa = 1.4$ . The normalized propagation constants  $\beta/k_0$  of all guided modes decrease monotonically as  $k_0a$  increases, i.e., dispersion curves

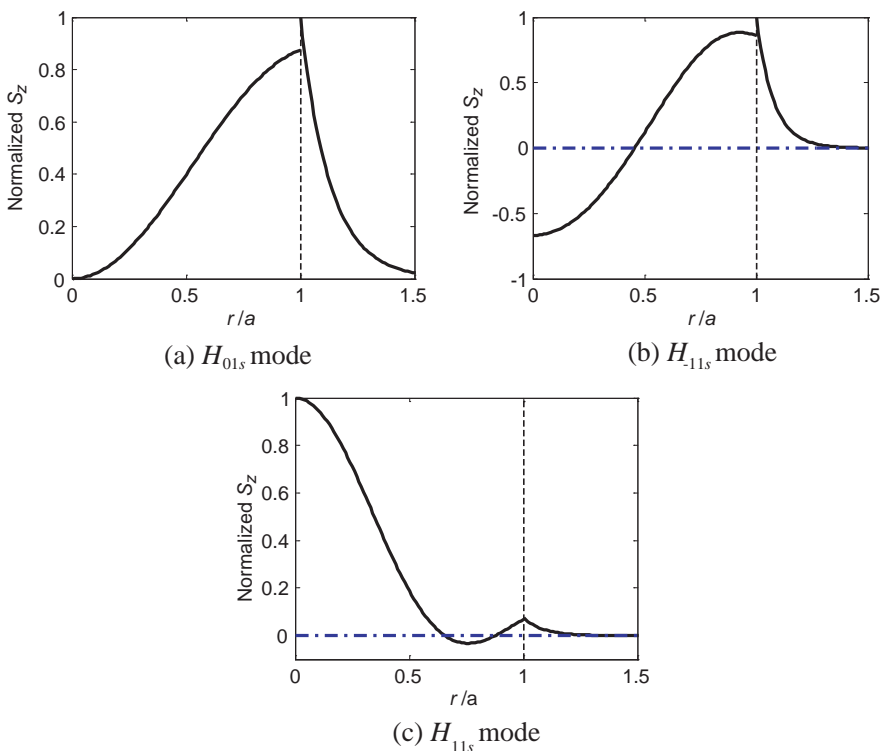


**Figure 3.** Normalized energy flux  $S_z$  of guided modes for  $\kappa = 2.0$  at  $k_0 a = 2.0$ .

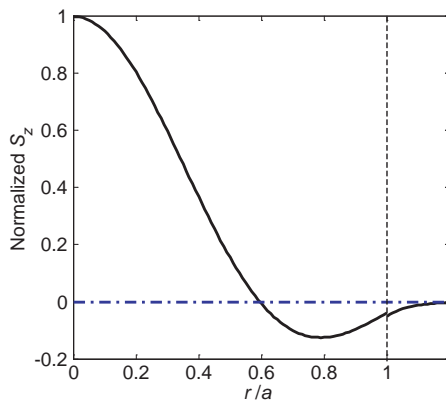


**Figure 4.** Normalized energy flux  $S_z$  of  $H_{11s}$  mode for  $\kappa = 2.0$  at  $k_0 a = 0.5$ .



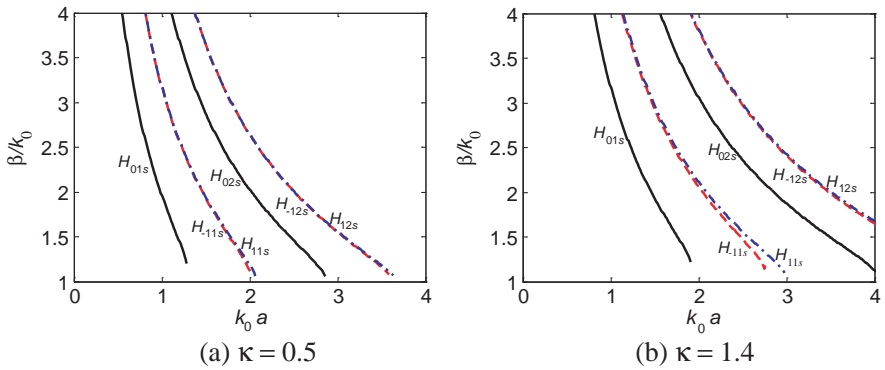


**Figure 5.** Dispersion curves of  $H_{01s}$ ,  $H_{-11s}$ ,  $H_{11s}$ ,  $H_{02s}$ ,  $H_{-12s}$ ,  $H_{12s}$  modes for different chirality parameters.

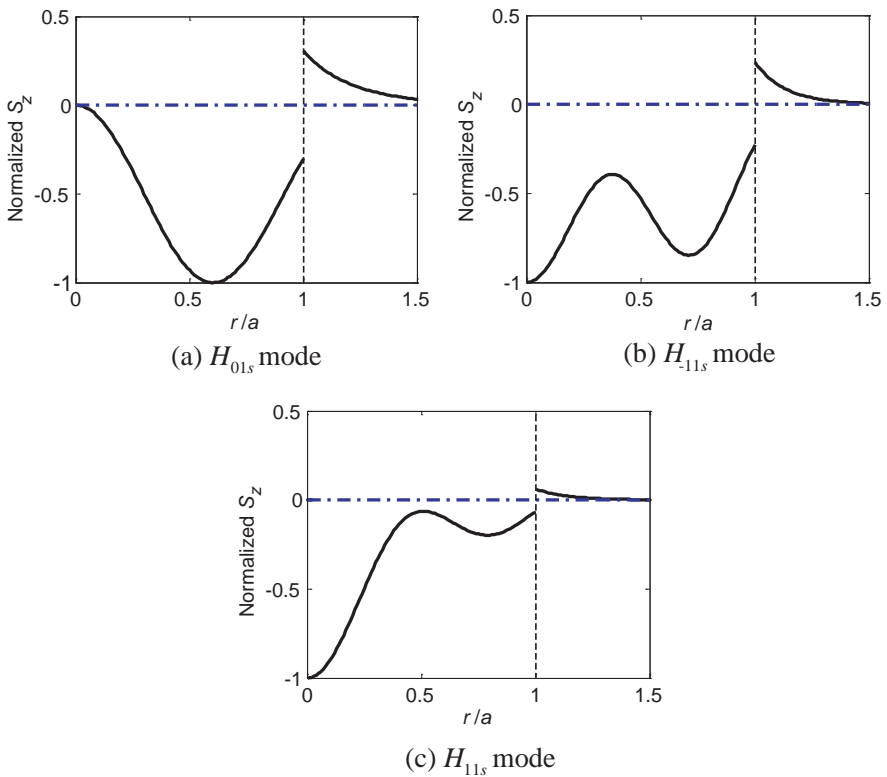


**Figure 6.** Normalized energy flux  $S_z$  of guided modes for  $\kappa = 0.5$  at  $k_0 a = 1.0$ .

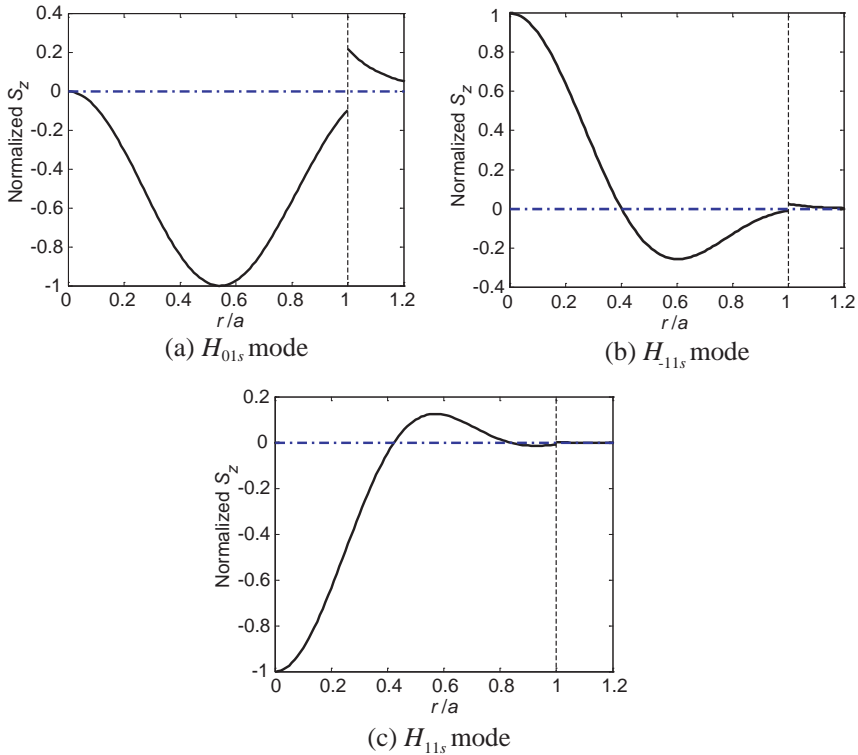


**Figure 7.** Normalized energy flux  $S_z$  of guided modes for  $\kappa = 1.4$  at  $k_0 a = 1.0$ .

of guided modes have negative slope.  $\beta/k_0$  are almost the same for different signs of  $m$  ( $H_{-11s}$  and  $H_{11s}$  modes,  $H_{-12s}$  and  $H_{12s}$  modes). The dispersion curves are similar even when  $\kappa$  approaches zero. When  $\kappa$  is very large, no solution of characteristic equation can be found.

The normalized energy flux  $S_z$  of  $H_{01s}$ ,  $H_{-11s}$  and  $H_{11s}$  modes at  $k_0 a = 1.0$  for  $\kappa = 0.5$  and  $\kappa = 1.4$  are plotted in Fig. 6 and Fig. 7. The energy flux  $S_z$  of all guided modes is negative in the core and positive in the cladding for  $\kappa = 0.5$ . However, for  $\kappa = 1.4$ , they are distinctly different. For  $H_{-11s}$  mode,  $S_z$  is positive near the center and negative near the interface in the core. For  $H_{11s}$  mode, there are three regions, near the center and interface,  $S_z$  are negative, and between these two regions,  $S_z$  is positive.

It is found that the normalized power  $P$  for all guided modes are negative, and the absolute value is smaller than one, which means that the power is negative in the core and positive in the cladding.

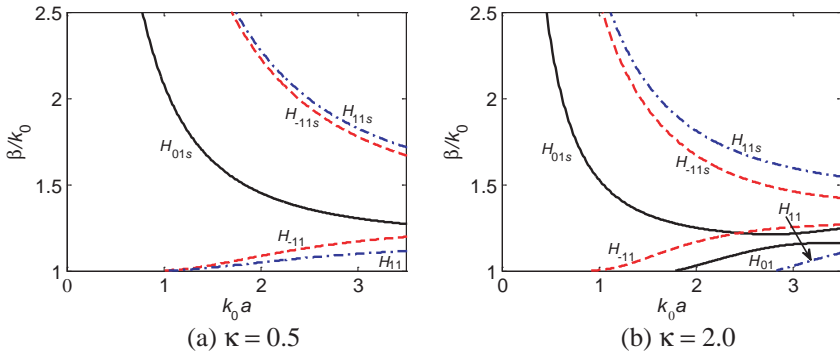


**Figure 8.** Dispersion curves of guided modes for different chirality parameters.

Thus these guided modes are backward waves, which means that the flow of the power is antiparallel to wave vector propagation direction, even if chirality parameter  $\kappa$  is very small or zero. This phenomenon is consistent with the result in the slab of uniaxial anisotropic media [37, 38]. This feature may have potential application in phase compensation or coupling devices.

### 3.3. Case III: $\varepsilon_t > 0, \varepsilon_z < 0$

We choose  $\varepsilon_t = 2\varepsilon_0, \varepsilon_z = -\varepsilon_0$ . Fig. 8 shows dispersion curves of guided modes for different chirality parameters  $\kappa = 0.5$  and  $\kappa = 2.0$ . The shapes of dispersion curves are similar as Fig. 1(b). There are other types of guided modes with negative slope shape even for  $\kappa$  approach zero. For chirality parameter  $\kappa = 0.5$  and  $\kappa = 2.0$  and smaller normalized frequency  $k_0 a$ , the energy flux  $S_z$  of guided modes are also similar as in Fig. 3 and Fig. 4. In this case, for all guided modes (including  $H_{mns}$  modes with negative slope curves), the normalized power  $P$  are always positive, thus they are also forward waves.

## 4. CONCLUSION

The characteristics of guided modes in the circular waveguide consist of uniaxial chiral medium have been investigated theoretically. The characteristic equation of guided modes is obtained. Numerical results for three kinds of uniaxial chiral media: I  $\varepsilon_t > 0, \varepsilon_z > 0$ , II  $\varepsilon_t < 0, \varepsilon_z > 0$ , and III  $\varepsilon_t > 0, \varepsilon_z < 0$  are presented. Effects of the chirality parameter on dispersion curves and energy flux of guided modes are discussed. Abnormal dispersion characteristics with negative slope

curves and negative energy flux in the core are found, i.e., backward wave is supported in the uniaxial chiral waveguide (even for chirality parameter approach zero) for  $\varepsilon_t < 0$ ,  $\varepsilon_z > 0$ . For  $\varepsilon_t > 0$ ,  $\varepsilon_z > 0$  and  $\varepsilon_t > 0$ ,  $\varepsilon_z < 0$ , there is negative energy flux even in the cladding. The results presented here will be helpful for potential applications in novel waveguide devices such as phase compensation or coupling devices. It is noted that we have neglected dispersion and losses of chiral media as done in [31–33]. However, usually chiral media are dispersive and lossy. It is a further work to study dispersive and lossy chiral waveguides in future.

## ACKNOWLEDGMENT

This work is supported by the National Natural Science Foundation of China (61078060), the Natural Science Foundation of Zhejiang Province, China (Y1091139), Ningbo Optoelectronic Materials and Devices Creative Team (2009B21007), and is partially sponsored by K. C. Wong Magna Fund in Ningbo University.

## REFERENCES

1. Tretyakov, S., I. Nefedov, A. Sihvola, S. Maslovski, and C. Simovski, "Waves and energy in chiral nihility," *Journal of Electromagnetic Waves and Applications*, Vol. 17, No. 5, 695–706, 2003.
2. Pendry, J. B., "A chiral route to negative refraction," *Science*, Vol. 306, 1353–1355, 2004.
3. Tretyakov, S., A. Sihvola, and L. Jylhä, "Backward-wave regime and negative refraction in chiral composites," *Photonics and Nanostructures*, Vol. 3, Nos. 2–3, 107–115, 2005.
4. Plum, E., J. Zhou, J. Dong, V. A. Fedotov, T. Koschny, C. M. Soukoulis, and N. I. Zheludev, "Metamaterial with negative index due to chirality," *Phys. Rev. B*, Vol. 79, 035407, 2009.
5. Zhang, S., Y. Park, J. Li, X. Lu, W. Zhang, and X. Zhang, "Negative refractive index in chiral metamaterials," *Phys. Rev. Lett.*, Vol. 102, 023901, 2009.
6. Zhou, J., J. Dong, B. Wang, T. Koschny, M. Kafesaki, and C. M. Soukoulis, "Negative refractive index due to chirality," *Phys. Rev. B*, Vol. 79, 121104(R), 2009.
7. Wiltshire, M. C. K., J. B. Pendry, and J. V. Hajnal, "Chiral Swiss rolls show a negative refractive index," *J. Phys. Condens. Matter*, Vol. 21, No. 29, 292201, 2009.

8. Dong, J., J. Zhou, T. Koschny, and C. M. Soukoulis, "Bi-layer cross chiral structure with strong optical activity and negative refractive index," *Optics Express*, Vol. 17, No. 16, 14172–14179, 2009.
9. Li, J., F.-Q. Yang, and J. Dong, "Design and simulation of L-shaped chiral negative refractive index structure," *Progress In Electromagnetics Research*, Vol. 116, 395–408, 2011.
10. Monzon, C. and D. W. Forester, "Negative refraction and focusing of circularly polarized waves in optically active media," *Phys. Rev. Lett.*, Vol. 95, 123904, 2005.
11. Jin, Y. and S. He, "Focusing by a slab of chiral medium," *Optics Express*, Vol. 13, No. 13, 4974–4979, 2005.
12. Jin, Y., J. He, and S. He, "Surface polaritons and slow propagation related to chiral media supporting backward waves," *Phys. Lett. A*, Vol. 351, Nos. 4–5, 354–358, 2006.
13. Dong, W., L. Gao, and C. W. Qiu, "Goos-Hänchen shift at the surface of chiral negative refractive media," *Progress In Electromagnetics Research*, Vol. 90, 255–268, 2009.
14. Dong, J. F., Z. J. Wang, L. L. Wang, and B. Liu, "Novel characteristics of guided modes in chiral negative refraction waveguides," *Proceedings of International Symposium on Biophotonics, Nanophotonics and Metamaterials, Metamaterials 2006*, 517–520, Oct. 2006.
15. Zhang, C. and T. J. Cui, "Chiral planar waveguide for guiding single-mode backward wave," *Opt. Commun.*, Vol. 280, No. 2, 359–363, 2007.
16. Dong, J. F., "Surface wave modes in chiral negative refraction grounded slab waveguides," *Progress In Electromagnetics Research*, Vol. 95, 153–166, 2009.
17. Dong, J. F. and J. Li, "Guided modes in the chiral negative refractive index fiber," *Chinese Optics Letters*, Vol. 8, No. 11, 1032–1036, 2010.
18. Cheng, Q. and C. Zhang, "Waves in planar waveguide containing chiral nihility metamaterial," *Opt. Commun.*, Vol. 276, No. 2, 317–321, 2007.
19. Qiu, C.-W., N. Burokur, S. Zouhdi, and L.-W. Li, "Chiral nihility effects on energy flow in chiral materials," *J. Opt. Soc. Am. A*, Vol. 25, 55–63, 2008.
20. Dong, J. and C. Xu, "Characteristics of guided modes in planar chiral nihility metamaterial waveguides," *Progress In Electromagnetics Research B*, Vol. 14, 107–126, 2009.

21. Dong, J. F. and C. Xu, "Surface polaritons in planar chiral nihility metamaterial waveguides," *Opt. Commun.*, Vol. 282, No. 19, 3899–3904, 2009.
22. Dong, J., "Exotic characteristics of power propagation in the chiral nihility fiber," *Progress In Electromagnetics Research*, Vol. 99, 163–178, 2009.
23. Dong, J. F., "Guided and surface modes in chiral nihility fiber," *Opt. Commun.* Vol. 283, No. 4, 532–536, 2010.
24. Dong, J., J. Li, and F.-Q. Yang, "Guided modes in the four-layer slab waveguide containing chiral nihility core," *Progress In Electromagnetics Research*, Vol. 112, 241–255, 2011.
25. Tuz, V. R. and C.-W. Qiu, "Semi-infinite chiral nihility photonics: Parametric dependence, wave tunneling and rejection," *Progress In Electromagnetics Research*, Vol. 103, 139–152, 2010.
26. Ahmed, S. and Q. A. Naqvi, "Electromagnetic scattering from a chiral-coated nihility cylinder," *Progress In Electromagnetics Research Letters*, Vol. 18, 41–50, 2010.
27. Cheng, X. X., H. S. Chen, X. M. Zhang, B. L. Zhang, and B.-I. Wu, "Cloaking a perfectly conducting sphere with rotationally uniaxial nihility media in monostatic radar system," *Progress In Electromagnetics Research*, Vol. 100, 285–298, 2010.
28. Naqvi, A., S. Ahmed, and Q. A. Naqvi, "Perfect electromagnetic conductor and fractional dual interface placed in a chiral nihility medium," *Journal of Electromagnetic Waves and Applications*, Vol. 24, Nos. 14–15, 1991–1999, 2010.
29. Naqvi, A., A. Hussain, and Q. A. Naqvi, "Waves in fractional dual planar waveguides containing chiral nihility metamaterial," *Journal of Electromagnetic Waves and Applications*, Vol. 24, Nos. 11–12, 1575–1586, 2010.
30. Baqir, M. A., A. A. Syed, and Q. A. Naqvi, "Electromagnetic fields in a circular waveguide containing chiral nihility metamaterial," *Progress In Electromagnetics Research M*, Vol. 16, 85–93, 2011.
31. Cheng, Q. and T. J. Cui, "Negative refractions in uniaxially anisotropic chiral media," *Phys. Rev. B*, Vol. 73, 113104, 2006.
32. Cheng, Q. and T. J. Cui, "Reflection and refraction properties of plane waves on the interface of uniaxially anisotropic chiral media," *J. Opt. Soc. Am. A*, Vol. 23, No. 12, 3203–3207, 2006.
33. Mahmoud, S. F. and A. J. Viitanen, "Modes in a hard surface waveguide with uniaxially anisotropic chiral material filling," *Progress In Electromagnetics Research*, Vol. 39, 265–279, 2003.

34. Qiu, R. C. and I.-T. Lu, "Guided waves in chiral optical fibers," *J. Opt. Soc. Am. A*, Vol. 11, No. 12, 3212–3219, 1994.
35. Mahmoud, S. F., "Guided modes on open chirowaveguides," *IEEE Trans. Microwave Theory Tech.*, Vol. 43, No. 1, 205–209, 1995.
36. Shadrivov, I. V., A. A. Sukhorukov, and Yu. S. Kivshar, "Guided modes in negative-refractive-index waveguides," *Phys. Rev. E* Vol. 67, 057602, 2003.
37. Lindell, I. V. and S. Ilvonen, "Waves in a slab of uniaxial BW medium," *Journal of Electromagnetic Waves and Applications*, Vol. 16, No. 3, 303–318, 2002.
38. Xu, G., T. Pan, T. Zhang, and J. Sun, "Characteristics of guided waves in indefinite-medium waveguides," *Opt. Commun.*, Vol. 281, No.10, 2819–2825, 2008.
39. Lindell, I. V., A. H. Sihvola, S. A. Tretyakov, and A. J. Viitanen, *Electromagnetic Waves in Chiral and Bi-Isotropic Media*, Artech House, Boston, London, 1994.